UAV Remote Sensing Technology for Wheat Growth Monitoring in Precision Agriculture: Comparison of Data Quality and Growth Parameter Inversion

Jikai Liu[1,2,3], Weiqiang Wang[1], Jun Li[1], Ghulam Mustafa[4], Xiangxiang Su[1], Ying Nian[1], Qiang Ma[1], Fengxian Zhen[5], Wenhui Wang[6], Xinwei Li[1,2,*]

[1] College of Resource and Environment, Anhui Science and Technology University, Fengyang, Anhui,China;
[2] Anhui Province Crop Intelligent Planting and Processing Technology Engineering Research Center, Fengyang, Anhui, China;
[3] National Engineering and Technology Center for Information Agriculture (NETCIA), Jiangsu Key Laboratory for Information Agriculture, Institute of Smart Agriculture, Nanjing Agricultural University, Nanjing, Jiangsu, China;
[4] Key Laboratory of Integrated Regulation and Resource Development on Shallow Lakes, Ministry of Education, College of Environment, Hohai University, Nanjing, China;
[5] College of Agriculture, Anhui Science and Technology University, Fengyang, Anhui,China;
[6] College of Life Science, Langfang Normal University, Langfang, Hebei, China.

* Correspondence: lixw@ahstu.edu.cn

Table S1. Vegetation indices (VIs) constructed by RGB images in this study

VIs	Formulas	References
b	$B/(B+G+R)$	Woebbecke et al., 1995
g	$G/(B+G+R)$	Woebbecke et al., 1995
r	$R/(B+G+R)$	Woebbecke et al., 1995
Excessive green index (ExG)	$2\times g-r-b$	Wyszecki and Stiles, 1968
Excessive red index (ExR)	$1.4\times r-g$	Meyer and Neto, 2008
Excess green minus excess red index (ExGR)	$3\times g-2.4\times r-\mathrm{b}$	Fu et al., 2020
Visible atmospherically resistant index (VARI)	$(G-R)/(G+R-B)$	Gitelson et al., 2002
Modified green blue vegetation index (MGRVI)	$(G^2-R^2)/(G^2+R^2)$	Bendig et al., 2015
Normalized green red difference index (NGRDI)	$(G-R)/(G+R)$	Hunt et al., 2005
Green red ratio index (GRRI)	G/R	Gamon and Surfus 1999
Vegetation index (VEG)	$g/r^{0.667}\times b^{0.333}$	Hague et al., 2006

B, G and R reflect the value of the Blue, Green and Red bands from RGB cameras, respectively.

Table S2. Vegetation indices (VIs) constructed by multispectral (MS) images in this study

VIs	Formulas	References
Modified green blue vegetation index (MGRVI)	$(green^2 - red^2)/(green^2 + red^2)$	Bendig et al., 2015
Normalized green red difference index (NGRDI)	$(green - red)/(green + red)$	Hunt et al., 2005
Green red ratio index (GRRI)	$green/red$	Gamon and Surfus 1999
Normalized difference vegetation index (NDVI)	$(nir - red)/(nir + red)$	Rouse et al., 1974
Normalized difference rededge index (NDRE)	$(nir - rededge)/(nir + rededge)$	Barnes et al., 2000
Leaf chlorophyll index (LCI)	$(nir - rededge)/(nir + red)$	Datt 1999
Green normalized difference vegetation index (GNDVI)	$(nir - green)/(nir + green)$	Gitelson et al., 1996
Ratio vegetation index (RVI)	nir/red	Jordan 1969
Rededge ratio vegetation index (RERVI)	$rededge/red$	Gitelson and Merzlyak, 1997
GM index (GM)	$rededge/green$	Gitelson and Merzlyak, 1997; Yan et al., 2005
Difference vegetation index (DVI)	$nir - red$	Tucker 1979
Red edge chlorophyll index (CIrededge)	$nir/rededge - 1$	Gitelson et al., 2003
Green chlorophyll index (CIgreen)	$nir/green - 1$	Gitelson et al., 2003
Soil adjusted vegetation index (SAVI)	$\frac{1.5\times(nir - red)}{nir + red + 0.5}$	Huete 1988
Optimized soil adjusted vegetation index (OSAVI)	$\frac{1.16\times(nir - red)}{nir + red + 0.16}$	Rondeaux et al., 1996
Modified soil adjusted vegetation index (MSAVI)	$\frac{((2\times nir+1) - ((2\times nir+1)^2 - 8\times(nir - red)))}{2}$	Qi et al., 1994
Green soil adjusted vegetation index (GSAVI)	$\frac{1.5\times(nir - green)}{nir + green + 0.5}$	Sripada et al., 2005
Atmospherically resistant vegetation index (ARVI)	$-0.18 + 1.17\times NDVI$	Kaufman and Tanre, 1992
Enhanced NDVI index (ENDVI)	$\frac{rededge + green - 2\times red}{rededge + green + 2\times red}$	Rasmussen et al., 2016
Renormalized difference vegetation index (RDVI)	$(nir - red)/\sqrt{(nir + red)}$	Roujean and Breon, 1995
Modified simple ratio (MSR)	$(RVI - 1)/\sqrt{RVI + 1}$	Chen, 1996
Anthocyanin reflectance index (ARI)	$nir\times(\frac{1}{green} - \frac{1}{rededge})$	Gitelson et al., 2006
MERIS terrestrial chlorophyll index (MTCI)	$(nir - rededge)/(rededge - red)$	Dash and Curran, 2004
Modified Vegetation Index (MVI)	$(rededge - red)/(nir + red)$	Su et al., 2024a
Near-infrared reflectance of vegetation (NIRv)	$NDVI\times nir$	Badgley et al., 2017
Rededge red normalized difference vegetation index (RERNDVI)	$(rededge - red)/(rededge + red)$	This study

blue, green, red, rededge and nir reflect the reflectance of the five multispectral bands from MS sensor, respectively.

Table S3. Description of texture features (TFs) used in this study

Texture features	Calculation equations	Features description
Mean(Mean)	$Mean = \sum_{i=1}^{N_g}\sum_{j=1}^{N_g} i \times P(i,j)$	The mean value in the GLCM window.
Variance(Var)	$Var = \sum_{i=1}^{N_g}\sum_{j=1}^{N_g} (i-u)^2 \times P(i,j)$	The variance in the GLCM window.
Homogeneity(Hom)	$Hom = \sum_{i=1}^{N_g}\sum_{j=1}^{N_g} \frac{1}{1+(i-j)^2} \times P(i,j)$	The homogeneity of grey level in the GLCM window.
Contrast(Con)	$Con = \sum_{i=1}^{N_g}\sum_{j=1}^{N_g} (i-j)^2 \times P(i,j)$	The clarity of texture in the GLCM window, as opposed to HOM.
Dissimilarity(Dis)	$Dis = \sum_{i=1}^{N_g}\sum_{j=1}^{N_g} \lvert i-j \rvert \times P(i,j)$	The similarity of the pixels in the GLCM window, similar to CON.
Entropy(Ent)	$Ent = -\sum_{i=1}^{N_g}\sum_{j=1}^{N_g} P(i,j) \times \log[P(i,j)]$	The diversity of the pixels in the GLCM window, proportional to the complexity of the image texture.
Second Moment(SM)	$SM = \sum_{i=1}^{N_g}\sum_{j=1}^{N_g} [P(i,j)]^2$	The uniformity of greyscale in the GLCM window.
Correlation(Cor)	$Cor = \frac{\sum_{i=1}^{N_g}\sum_{j=1}^{N_g} (i,j) \times P(i,j) - u_i u_j}{\sigma_i \sigma_j}$	The linear dependency of greyscale on those of neighboring pixels in the GLCM window.

P(i,j) represents the probability of each pixel pair (i ,j) value and i, j are the gray tones in the windows, which are also the coordinates of the co-occurrence matrix space; Ng represents the number of distinct grey levels in the quantized image, which has a gray value range of the original image; μ and σ represents the mean and standard deviation of P(i,j), respectively.

Table S4. Pixel-scale image quality assessment metrics used in this study

PIQA metrics	Equations	Descriptions	References
CC	$\frac{\sum_1^M \sum_1^N (f-\overline{f})(g-\overline{g})}{\sqrt{\sum_1^M \sum_1^N (f-\overline{f})^2 \sum_1^M \sum_1^N (g-\overline{g})^2}}$	Analyze the spectral similarity between corresponding comparative images.	Shah et al. 2019
PSNR	$10 \bullet \log_{10}(Max^2/MSE)$	The ratio between the maximum possible signal value and the noise, with higher values indicating better quality.	Hore and Ziou, 2010
RMSE	$\sqrt{\frac{1}{MN}\sum_{i=1}^{M}\sum_{j=1}^{N}(g(i,j)-f(i,j))^2}$	The mean squared error between the original image and the processed image, with smaller values indicating higher quality.	Samajdar and Quraishi, 2015
AG	$\frac{\sum_{i=1}^{M-1}\sum_{j=1}^{N-1}\sqrt{[f(i,j)-f(i+1,j)]^2+[f(i,j)-f(i,j+1)]^2}/2}{(M-1)(N-1)}$	The average degree of change in pixel intensity values in an image, reflecting the image's clarity or level of detail.	Sun et al. 1998
H	$-\sum_{k=0}^{G-1} P_k \log_2 P_k$	The amount of information in an image, with higher values typically indicating that the more information.	Shannon, 1948

f(i,j) and g(i,j) represent the pixel values at the i-th row and j-th column of the images to be compared, respectively. M and NNN represent the number of rows and columns in the image. Max and MSE represent the dynamic range of image pixels and the mean squared error, respectively. Pk is the probability distribution of the pixel intensity value k in the image. G is the pixel values level in the image.

Table S5. Results of machine learning inversion models for wheat growth parameters based on RGB image sensitive features from two UAV platforms

Parameters	platforms	ML	SFs				TFs				SFs+TFs			
			R^2	R^2_CV(%)	rRMSE(%)	rRMSE_CV(%)	R^2	R^2_CV(%)	rRMSE(%)	rRMSE_CV(%)	R^2	R^2_CV(%)	rRMSE(%)	rRMSE_CV(%)
AGB	M2P	ELM	0.73	14.77	38.63	26.16	0.77	10.51	35.07	16.76	0.83	5.47	29.95	14.05
		GPR	0.71	7.44	39.29	9.55	0.77	8.63	34.99	14.09	0.81	6.32	32.10	11.78
		PLSR	0.72	7.61	38.77	10.54	0.80	8.09	33.13	16.39	0.85	6.42	28.40	17.39
		RF	0.77	8.26	35.22	12.83	0.62	17.85	45.62	13.18	0.79	7.82	34.34	12.12
		SVR	0.79	5.92	35.03	12.42	0.70	13.63	42.44	12.66	0.81	5.20	33.76	12.21
	M3M	ELM	0.69	12.53	41.68	23.59	0.73	11.09	37.49	14.69	0.74	11.32	37.50	16.03
		GPR	0.66	9.46	42.50	9.81	0.73	12.50	37.48	14.99	0.77	8.83	35.16	15.16
		PLSR	0.65	9.09	43.75	13.99	0.71	11.93	39.46	13.79	0.76	9.84	35.92	16.43
		RF	0.74	9.31	37.1	13.62	0.76	10.01	36.95	14.82	0.76	7.79	36.53	11.83
		SVR	0.72	11.10	39.53	17.10	0.75	9.95	38.56	12.93	0.78	7.02	35.94	14.34
PNC	M2P	ELM	0.71	18.15	18.78	21.54	0.64	18.78	20.85	13.55	0.83	5.24	14.19	12.82
		GPR	0.50	25.71	24.67	10.40	0.63	14.96	20.92	9.65	0.72	11.74	18.07	10.75
		PLSR	0.52	23.87	24.31	11.27	0.67	17.08	19.63	14.71	0.84	7.12	13.65	15.93
		RF	0.71	13.54	18.11	13.07	0.54	22.91	23.31	14.01	0.72	12.36	18.39	10.99
		SVR	0.78	8.54	15.87	10.55	0.52	23.19	23.85	11.63	0.80	8.12	15.40	13.07
	M3M	ELM	0.60	18.69	22.23	19.38	0.56	27.53	23.34	19.69	0.64	15.52	20.79	14.53
		GPR	0.53	26.15	23.82	11.87	0.53	19.19	23.56	8.10	0.58	21.66	22.06	11.24
		PLSR	0.55	23.55	23.06	12.11	0.49	26.65	25.25	14.72	0.57	25.57	22.43	15.46
		RF	0.73	14.63	17.70	14.75	0.57	18.14	22.55	10.11	0.74	13.54	17.29	14.19
		SVR	0.72	14.48	17.83	14.91	0.61	18.78	21.20	11.74	0.77	11.56	16.22	16.41
SPAD	M2P	ELM	0.57	22.37	8.15	12.03	0.54	23.00	8.44	10.02	0.55	23.04	8.43	13.19
		GPR	0.56	21.99	8.13	11.03	0.56	22.59	8.15	11.55	0.56	22.58	8.17	10.85

	PLSR	0.56	22.40	8.19	11.19	0.55	22.86	8.28	10.86	0.55	22.84	8.26	11.27
	RF	0.62	20.07	7.61	12.55	0.56	22.64	8.16	11.52	0.60	19.43	7.72	10.85
	SVR	0.61	18.27	7.64	12.05	0.56	21.15	8.17	13.35	0.60	17.33	7.78	13.08
	ELM	0.49	26.52	9.30	22.07	0.52	24.48	8.56	10.56	0.52	28.65	8.65	13.90
	GPR	0.43	25.21	9.47	12.08	0.54	23.22	8.33	9.91	0.53	22.43	8.45	10.56
M3M	PLSR	0.44	27.51	9.37	12.33	0.53	23.19	8.45	9.86	0.52	24.57	8.52	10.91
	RF	0.56	19.65	8.40	10.67	0.51	27.24	8.63	10.10	0.59	18.44	7.87	9.98
	SVR	0.57	19.81	8.18	13.09	0.53	24.62	8.44	11.97	0.60	17.34	7.80	13.14

CV: Coefficient of Variation, the percentage of the quotient between the mean and the standard deviation. ML:machine learning inversion models.

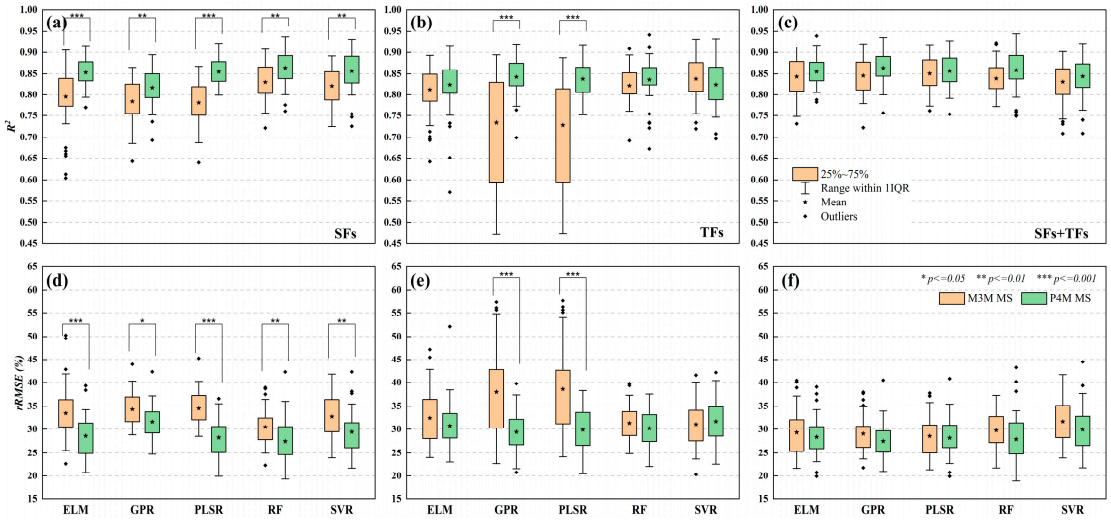

Figure S1. AGB inversion results of machine learning models based on MS image sensitive features from two UAV platforms.(a)–(c) represented the R^2 values of the inversion models, while (d)–(f) were the rRMSE values of the inversion models. (a, d) show results based on the SFs feature, (b, e) show results based on the TFs feature, and (c, f) show results based on the combined SFs+TFs feature.

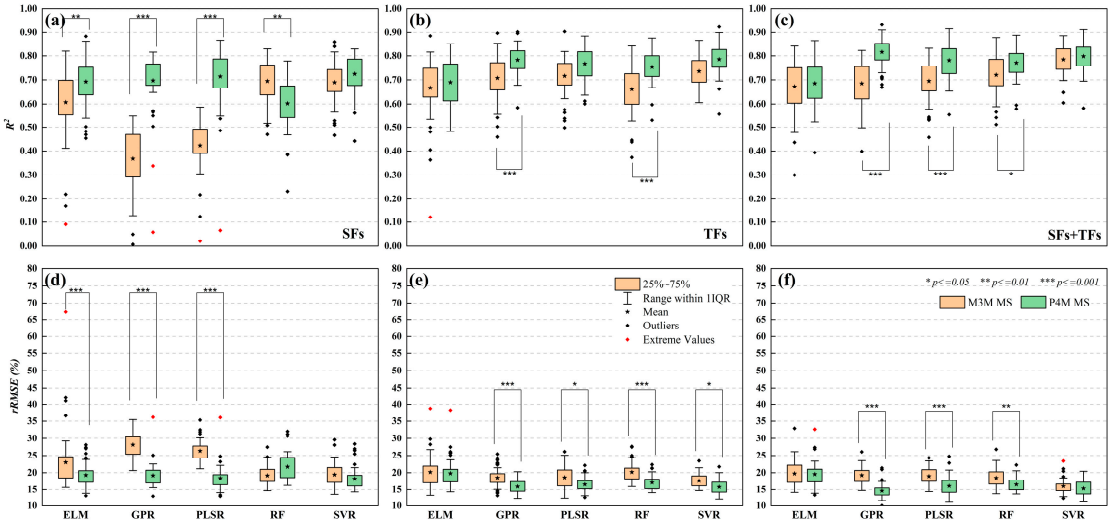

Figure S2. PNC inversion results of machine learning models based on MS image sensitive features from two UAV platforms.(a)–(c) represented the R^2 values of the inversion models, while (d)–(f) were the rRMSE values of the inversion models. (a, d) show results based on the SFs feature, (b, e) show results based on the TFs feature, and (c, f) show results based on the combined SFs+TFs feature.

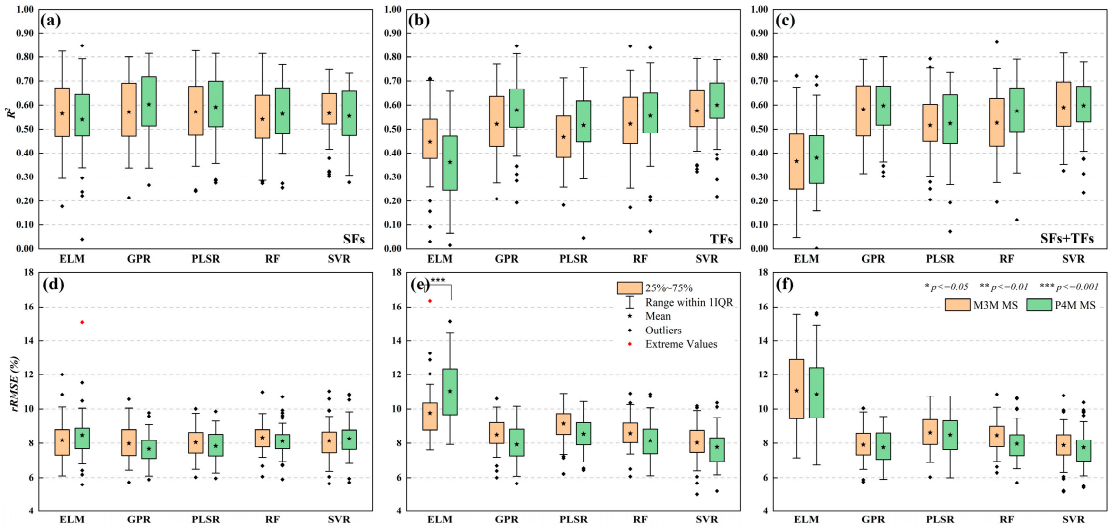

Figure S3. SPAD inversion results of machine learning models based on MS image sensitive features from two UAV platforms.(a)–(c) represented the R^2 values of the inversion models, while (d)–(f) were the rRMSE values of the inversion models. (a, d) show results based on the SFs feature, (b, e) show results based on the TFs feature, and (c, f) show results based on the combined SFs+TFs feature.

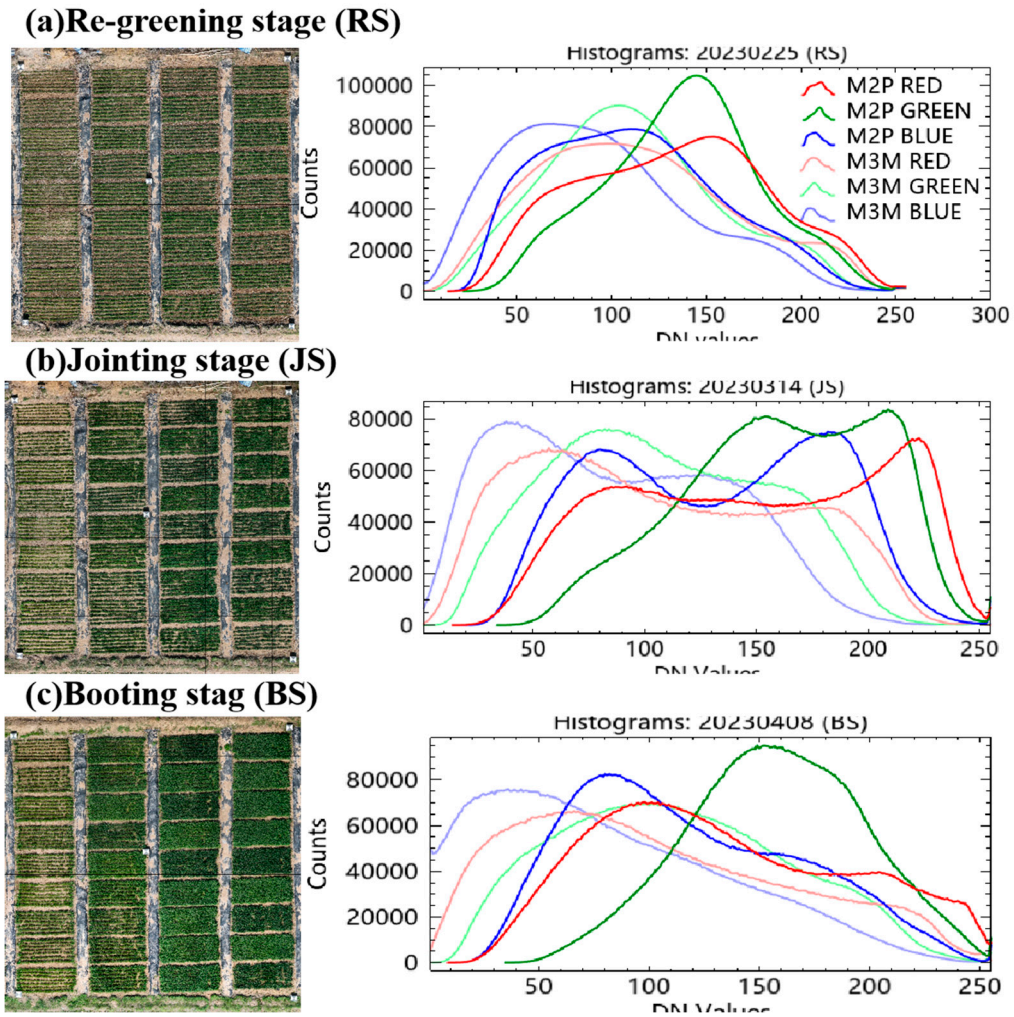

Figure S4. Grayscale histogram of different UAV-based RGB cameras at three critical growth stages.

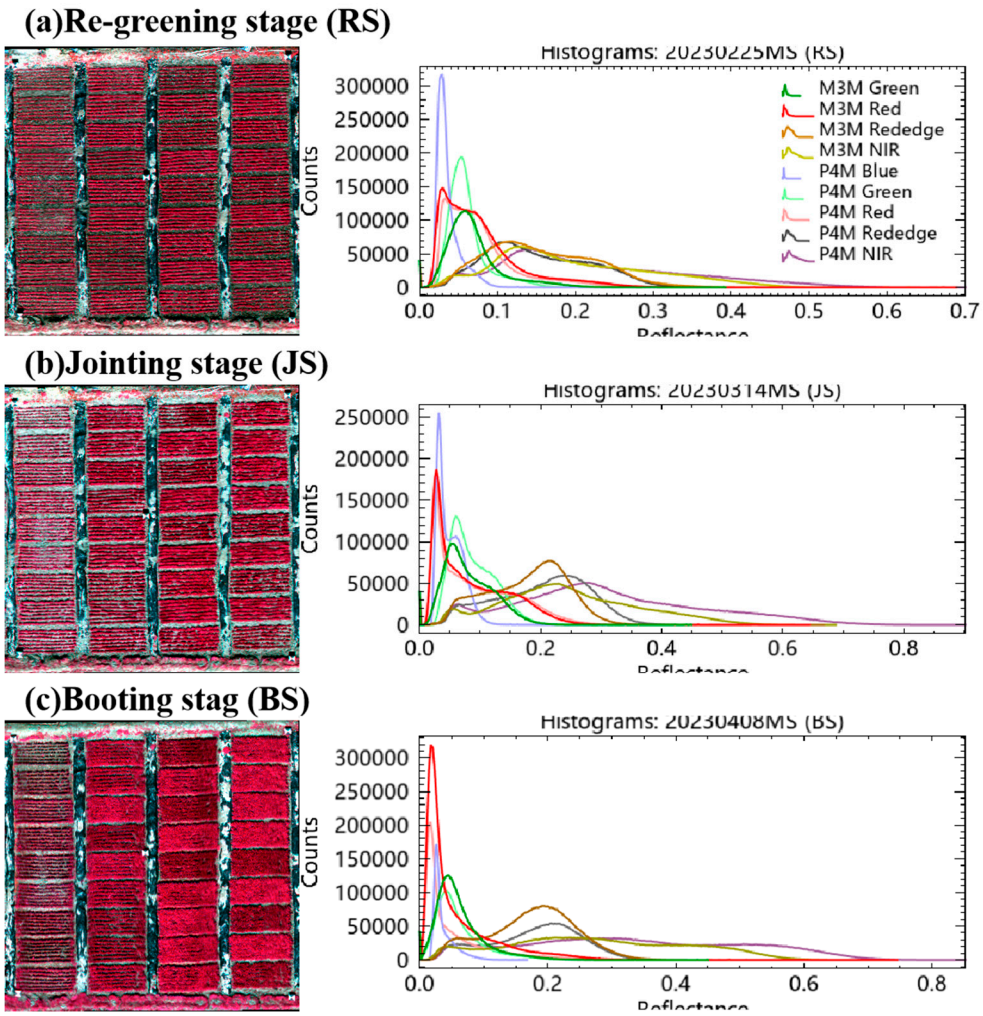

Figure S5. Grayscale histogram of different UAV-based MS sensors at three critical growth stages.

References

Badgley, G., Field, C.B. and Berry, J.A. 2017. Canopy Near-Infrared Reflectance and Terrestrial Photosynthesis. Sci. Adv. 3 (3), e1602244. https://doi.org/10.1126/sciadv.1602244.

Barnes, E., Clarke, T., Richards, S., et al. 2000. Coincident detection of crop water stress, nitrogen status and canopy density using ground based multispectral data. Proceedings of the 5th international conference on precision agriculture, ASA-CSSA-SSSA, Bloomington, MN, USA. https://www.tucson.ars.ag.gov/unit/publications/PDFfiles/1356.pdf. (Accept Oct. 11 2024).

Bendig, J., Yu, K., Aasen, H., et al. 2015. Combining UAV-based plant height from crop surface models, visible, and near infrared vegetation indices for biomass monitoring in barley. Int. J. Appl. Earth Obs. Geoinf. 39, 79–87. https://doi.org/10.1016/j.jag.2015.02.012.

Chen J M. 1996. Evaluation of vegetation indices and a modified simple ratio for boreal applications. Canadian Journal of Remote Sensing, 22(3): 229-242. https://doi.org/10.1080/07038992.1996.10855178.

Dash, J. and Curran, P.J., 2004. The MERIS Terrestrial Chlorophyll Index. INT J REMOTE SENS. 25, pp. 5003–5013. https://doi.org/10.1080/0143116042000274015.

Datt, B. 1999. A new reflectance index for remote sensing of chlorophyll content inhigher plants: tests using Eucalyptus leaves. J. Plant Physiol. 154, 30–36. https://doi.org/10.1016/S0176-1617(99)80314-9.

Fu, Y., Yang, G., Li, Z., et al. 2020. Winter wheat nitrogen status estimation using UAV-based RGB imagery and

Gaussian processes regression. Remote Sens. 12, 3778–3805. https://doi.org/10.3390/rs12223778.

Gamon, J.A. and Surfus, J.S. 1999. Assessing leaf pigment content and activity with a reflectometer. New Phytol. 143, 105–117. https://doi.org/10.1046/j.1469-8137.1999.00424.x.

Gitelson, A. A. and Merzlyak, M. N. 1997. Remote estimation of chlorophyll content in higher plant leaves. International journal of remote sensing,18(12): 2691-2697. https://doi.org/10.1080/014311697217558.

Gitelson, A. A., Gritz, Y., and Merzlyak, M. N. 2003. Relationships between leaf chlorophyll content and spectral reflectance and algorithms for nondestructive chlorophyll assessment in higher plant leaves. J. Plant Physiol. 160,271–282. doi: 10.1078/0176-1617-00887.

Gitelson, A. A., Kaufman, Y. J., and Merzlyak, M. N. 1996. Use of a green channel in remote sensing of global vegetation from EOS-MODIS. Remote Sens.Environ. 58, 289–298. doi: 10.1016/S0034-4257(96)00072-7.

Gitelson, A. A., Kaufman, Y. J., Stark, R., et al. 2002. Novel algorithms forremote estimation of vegetation fraction. Remote Sens. Environ. 80(1),76–87. https://doi.org/10.1016/S0034-4257(01)00289-9.

Gitelson, A. A., Keydan, G. P. and Merzlyak, M. N. 2006. Three-band model for noninvasive estimation of chlorophyll, carotenoids, and anthocyanin contents in higher plant leaves. Geophysical research letters, 33(11). https://doi.org/10.1029/2006GL026457.

Hague, T., Tillett, N.D. and Wheeler, H. 2006. Automated crop and weed monitoring in widely spaced cereals. Precis.Agric. 7, 21–32.https://doi.org/10.1007/s11119-005-6787-1.

Hore, A.; Ziou, D. 2010. Image quality metrics: PSNR vs. SSIM[C]. 20th international conference on pattern recognition. IEEE: 2366-2369. doi:10.1109/ICPR.2010.579.

Huete, A.R. 1988. A Soil-Adjusted Vegetation Index (SAVI). Remote Sens. Environ. 25 (3), 295–309. https://doi.org/10.1016/0034-4257(88)90106-X.

Hunt, E.R., Cavigelli, M., Daughtry, C.S.T., et al. 2055. Evaluation of digital photography from model aircraft for remote sensing of crop biomass and nitrogen status. Precis. Agric. 6, 359–378. https://doi.org/10.1007/s11119-005-2324-5.

Kaufman, Y .J.; Tanre, D. 1992. Atmospherically resistant vegetation index (ARVI) for EOS-MODIS.Ieee Trans.Geosci. Remote Sens., 30, 261–270. DOI: 10.1109/36.134076.

Meyer, G.E. and Neto, J.C. 2008. Verification of color vegetation indices for automated crop imaging applications. Comput. Electron. Agric. 63, 282–293. https://doi.org/10.1016/j.compag.2008.03.009.

Qi, J., Chehbouni, A., Huete, A. R., et al. 1994. A modifed adjusted vegetation index (MSAVI). Remote Sens. Environ. 48, 119–126. https://doi.org/10.1016/0034-4257(94)90134-1.

Rasmussen, J., Ntakos, G., Nielsen, J., et al. 2016. Are vegetation indices derived from consumer-grade cameras mounted on UA Vs sufficiently reliable for assessing experimental plots? Eur. J. Agron.74, 75–92. https://doi.org/10.1016/j.eja.2015.11.026.

Rondeaux, G., Steven, M. and Baret, F., 1996. Optimization of soil-adjusted vegetation indices. Remote Sens. Environ. 55, 95–107. https://doi.org/10.1016/0034-4257(95)00186-7.

Roujean, J. L. and Breon, F. M. 1995. Estimating PAR absorbed by vegetation from bidirectional reflectance measurements. Remote sensing of Environment, 51(3): 375-384. https://doi.org/10.1016/0034-4257(94)00114-3.

Rouse, J. W., Haas, R. H., Schell, J. A., et al. 1974. Monitoring vegetation systems in the Great Plains with ERTS. NASA. Goddard Space Flight Center 3d ERTS-1 Symphony. 1, Section A, 309–317. Washington, DC, USA. https://ntrs.nasa.gov/citations/19740022614. (Accept Oct. 11 2024).

Samajdar, T.; Quraishi, M.I. 2015. Analysis and Evaluation of Image Quality Metrics. In: Mandal, J., Satapathy, S., Kumar Sanyal, M., Sarkar, P., Mukhopadhyay, A. (eds) Information Systems Design and Intelligent Applications. Advances in Intelligent Systems and Computing, 340. Springer, New Delhi. https://doi.org/10.1007/978-81-322-2247-7_38.

Shah, E.; Jayaprasad, P.; and James, M.E. 2019. Image fusion of SAR and optical images for identifying antarctic ice features. Journal of the Indian Society of Remote Sensing, 47 (12):2113–2127. doi:10.1007/s12524-019-01040-3.

Shannon, C. E. 1948. A mathematical theory of communication. The Bell system technical journal, 27(3): 379-423. doi:10.1002/j.1538-7305.1948.tb01338.x.

Sripada, R.P., Heiniger, R.W., White, J.G., et al. 2005. Aerial color infrared photography for determining late-season nitrogen requirements in corn. Agron. J. 97, 1443–1451. https://doi.org/10.2134/agronj2004.0314.

Su, X., Nian, Y., Shaghaleh, H., et al. 2024a. Combining features selection strategy and features fusion strategy for SPAD estimation of winter wheat based on UAV multispectral imagery. Frontiers in Plant Science

15:1404238. doi: 10.3389/fpls.2024.1404238.

Sun, J.; Liu, J.; Li, J. 1998. Multi-source remote sensing image data fusion. Journal of remote sensing, 2(01):47-50. doi:CNKI:SUN:YGXB.0.1998-01-008. (In chinese).

Tucker, C.J., 1979. Red and photographic infrared linear combinations for monitoring vegetation. Remote Sens. Environ. 8, 127–150. https://doi.org/10.1016/0034-4257(79)90013-0.

Woebbecke, D.M., Meyer, G.E., B.K., V., et al. 1995. Color indices for weed identification under various soil, residue and lighting conditions. Transactions of the ASAE 38, 259–269. DOI:10.13031/2013.27838.

Wyszecki, G.W. and Stiles, W.S., 1968. Color Science: Concepts and Methods, Quantitative Data and Formulae. Phys. Today. 21, 83–84. https://doi.org/10.2307/1420820.

Yan C., Niu Z., Wang J., et al. 2005. The assessment of spectral indices applied in chlorophyll content retrieval and a modified crop canopy chlorophyll content retrieval model. Journal of remote sensing,9(6):742-750. DOI： 10.11834/jrs.200506107 . (In Chinese).